International Journal of Engineering, Mathematical and Physical Sciences
ISSN: 2517-9934
Vol:9, No:4, 2015

Numerical Modeling of the Depth-Averaged Flow Over a Hill

Anna Avramenko, Heikki Haario

Abstract—This paper reports the development and application of a 2D[1] depth-averaged model. The main goal of this contribution is to apply the depth averaged equations to a wind park model in which the treatment of the geometry, introduced on the mathematical model by the mass and momentum source terms. The depth-averaged model will be used in future to find the optimal position of wind turbines in the wind park. $\kappa - \varepsilon$ and 2D LES turbulence models were consider in this article. 2D CFD[2] simulations for one hill was done to check the depth-averaged model in practise.

Keywords—Depth-averaged equations, numerical modeling, CFD

I. Introduction

THE depth-averaged equations are obtained, as the name suggests, by averaging the Reynolds equations over the depth. The following conditions have to be met in order for the depth-averaged model to be applicable:

- the vertical momentum exchange is negligible and the vertical velocity component *w* is a lot smaller than the horizontal components *u* and *v*.
- the pressure gain is linear with the depth.

The goal of this method is to reduce the elapsed time of CFD simulations from hours to minutes. Depth-averaged equations have been used for high Reynolds number turbulent water flows and mostly for open channels like in the modelling of a tidal flow in complex estuaries [6] and for water flows in a lake or in a sea [10]. Depth-averaged equations have been validated also for flows in a closed channel, such as in a headbox of a paper machine [5], [4]. In simulating such flows there normally exist many difficulties like a complex geometry, the size of domain and different length scales. Thus it is very difficult to have a fine mesh for a boundary layers to achieve a sufficient resolution. Hence, depth-averaged model are a good approach for this kind of flow simulations and sometimes it provides even more accurate solutions than 3D [7].

The general idea of the current research is to use the depth-averaged equations for the wind park model. The goal is to optimize a location of wind turbines for the best results. But 3D simulation takes a lot of times that is why it was decided to consider the 2D simulation by using the depth-averaged model. Turbines will be taken into account in 2D simulation by using actuator disks. But firstly, steady-state Navier-Stokes equations was consider and the depth-averaged model was applied for the hill. The results are presented in this paper.

A. Avramenko is with the Department of Mathematics and Physics, Lappeenranta University of Technology, Lappeenranta, 53851 Finland, e-mail: Anna.Avramenko@lut.fi.
H. Haario is with Lappeenranta University of Technology.

[1]Two-dimensional
[2]Computational Fluid Dynamics

II. Depth-Averaged Governing Equations

Steady-state Navier-Stokes equations for incompressible flow are:

$$\nabla \cdot \vec{v} = 0 \tag{1}$$

$$\rho \nabla \cdot (\vec{v}\vec{v}) = -\nabla p + \nabla \cdot (\bar{\bar{\tau}}) \tag{2}$$

where the tensor $\bar{\bar{\tau}}$ is given by

$$\bar{\bar{\tau}} = \mu \left[\left(\nabla \vec{v} + \nabla \vec{v}^T \right) - \frac{2}{3} \nabla \cdot \vec{v} I \right], \tag{3}$$

$\vec{v} = (u, v, z)$ is the velocity vector, p is pressure and ρ - density. The depth-averaging will be performed along the z-direction between the bottom level $d_1(x, y)$ and the top level $d_2(x, y)$. The depth-averaged $U(x, y)$ and $V(x, y)$ velocity components are thus defined as:

$$U = \frac{1}{D} \int_{d_1}^{d_2} u dz \quad \text{and} \quad V = \frac{1}{D} \int_{d_1}^{d_2} v dz \tag{4}$$

where $D(x, y) = d_2(x, y) - d_1(x, y)$ is the depth of the chanel.

The geometry will be represented by long parallelepiped, where bottom surface is rough surface (represents ground) and top surface is straight one, that means $d_2(x, y) = const$.

The symmetry boundary condition on the top means that

$$\frac{\partial u}{\partial z} = 0, \ \frac{\partial v}{\partial z} = 0, \ w = 0, \ \frac{\partial d_2}{\partial x} = 0, \ \frac{\partial d_2}{\partial y} = 0, \ \frac{\partial d_2}{\partial z} = 0 \tag{5}$$

The wall boundary condition on the ground can be expressed in the next form:

$$u(x, y, d_1) = 0, \ v(x, y, d_1) = 0, \ w(x, y, d_1) = 0 \tag{6}$$

Assuming that gravity is insignificant, the pressure can be approximated as a constant in the z-direction.

1) Continuty equation: Integrating the continuty equation along the depth, using the Leibnitz rule:

$$\frac{\partial}{\partial t} \int_{a(y,t)}^{b(y,t)} f(x, y, t) dx = \int_{a(y,t)}^{b(y,t)} \frac{\partial f}{\partial t} dx - f(a, y, t) \frac{\partial a}{\partial t} + f(b, y, t) \frac{\partial b}{\partial t} \tag{7}$$

and the boundary conditions (5), (6), the continuty equation becomes

$$\rho \left(\frac{\partial}{\partial x} (DU) + \frac{\partial}{\partial y} (DV) \right) = 0 \tag{8}$$

According to this equation, mass source can be written as

$$\rho\left(\frac{\partial U}{\partial x}+\frac{\partial V}{\partial y}\right)=-\frac{\rho}{D}\left(\frac{\partial D}{\partial x}U+\frac{\partial D}{\partial y}V\right)=S_{mass} \quad (9)$$

2) Momentum equation in the x-direction: When the momentum equation in the x-direction is integrated along the depth z, one obtains

$$\rho\int_{d_1}^{d_2}\left(\frac{\partial(uu)}{\partial x}+\frac{\partial(uv)}{\partial y}+\frac{\partial(uw)}{\partial z}\right)dz= \\ -\int_{d_1}^{d_2}\frac{\partial p}{\partial x}dz+\int_{d_1}^{d_2}\left(\frac{\partial \tau_{xx}}{\partial x}+\frac{\partial \tau_{xy}}{\partial y}+\frac{\partial \tau_{xz}}{\partial z}\right)dz \quad (10)$$

The first convection term - the first term in the left-hand side of (10) - gives

$$\int_{d_1}^{d_2}\frac{\partial u^2}{\partial x}dz= \\ \frac{\partial}{\partial x}\int_{d_1}^{d_2}u^2dz-u^2(x,y,d_2)\frac{\partial d_2}{\partial x}+u^2(x,y,d_1)\frac{\partial d_1}{\partial x} \quad (11)$$

The last two terms in the right-hand side equals zero because of boundary conditions. The integration of the velocity product u^2 does not give the square of the depth-averaged velocity U. Several authors suggest to use the Boussinesq coefficient β in order to take into account this difference [3], [1]:

$$\int_{d_1}^{d_2}u^2dz=\beta_{xx}U^2D \quad (12)$$

Usually authors assume that Boussinesq coefficients equal $\beta_{xx}=\beta_{xy}=1$, neglecting thus the dispersion effect [2]. Returning to (11), it finally gives

$$\int_{d_1}^{d_2}\frac{\partial u^2}{\partial x}dz=\frac{\partial}{\partial x}\left(U^2D\right) \quad (13)$$

The pressure term in equation (10) can be written as:

$$\int_{d_1}^{d_2}\frac{\partial p}{\partial x}dz=\frac{\partial p}{\partial x}D \quad (14)$$

The stress tensor with the tensor notation is defined as:

$$\tau_{ij}=\mu\left[\left(\frac{\partial u_i}{\partial x_j}+\frac{\partial u_j}{\partial x_i}\right)-\frac{2}{3}\delta_{ij}\frac{\partial u_k}{\partial x_k}\right] \quad (15)$$

Other directional terms in (15) are handled with the help of simulated depth-averaged velocities, except τ_{i3}, where $i=1,2$, which means the z direction.

$$\frac{1}{D}\int_{d_1}^{d_2}\frac{\partial \tau_{i3}}{\partial z}dz=\frac{1}{D}[\tau_{i3}(d_2)-\tau_{i3}(d_1)], i=1,2 \quad (16)$$

$$\tau_{13}=\mu\frac{\partial u_1}{\partial z}+\mu\frac{\partial u_3}{\partial x}=\mu\frac{\partial u_1}{\partial z} \quad (17)$$

$$\tau_{23}=\mu\frac{\partial u_2}{\partial z}+\mu\frac{\partial u_3}{\partial y}=\mu\frac{\partial u_2}{\partial z} \quad (18)$$

Velocity components u_1 and u_2 can be defined with the help of the average velocities U_1, U_2, and the z-directional velocity profile S [8]

$$u_1(x,y,z)=U_1(x,y)S(z) \quad (19)$$

$$u_2(x,y,z)=U_2(x,y)S(z) \quad (20)$$

$$S(z)=\frac{n+1}{n}\left(1-|1-\frac{2}{D}z|^n\right) \quad (21)$$

$n=2$ for laminar flow and $n=7$ for turbulent flow. Hence, the friction terms for x_1 and x_2 components can be written as

$$\tau_{i3}=-\frac{4\mu U_i(n+1)}{D^2} \quad (22)$$

Finaly, grouping again all terms of (10), depth-averaged momentum equation in the x-direction can be written as

$$\rho\left(\frac{\partial(uu)}{\partial x}+\frac{\partial(uv)}{\partial y}\right)= \\ -\frac{\partial p}{\partial x}+\left(\frac{\partial \tau_{xx}}{\partial x}+\frac{\partial \tau_{xy}}{\partial y}\right)+US_{mass}-\frac{32\mu U}{D^2} \quad (23)$$

3) Momentum equation in the y-direction: By analogy, momentum equation in the y-direction can be presented as follows

$$\rho\left(\frac{\partial(uv)}{\partial x}+\frac{\partial(vv)}{\partial y}\right)= \\ -\frac{\partial p}{\partial y}+\left(\frac{\partial \tau_{xy}}{\partial x}+\frac{\partial \tau_{yy}}{\partial y}\right)+VS_{mass}-\frac{32\mu V}{D^2} \quad (24)$$

The Y momentum source becomes:

$$S_{my}=VS_{mass}-\frac{32\mu V}{D^2} \quad (25)$$

4) Source terms for depth-averaged $\kappa-\varepsilon$ model: The simplified production terms for turbulence and its dissipation are similar to [9] since the κ and ε equations cannot be integrated over the height so that they assume a closed form (25), (26).

$$\frac{\partial k}{\partial t}+U\frac{\partial k}{\partial x}+V\frac{\partial k}{\partial y}= \\ \frac{\partial}{\partial x}\left(\frac{\nu_t}{\sigma_k}\frac{\partial k}{\partial x}\right)+\frac{\partial}{\partial y}\left(\frac{\nu_t}{\sigma_k}\frac{\partial k}{\partial y}\right)+P_h+P_{k\nu}-\epsilon \quad (26)$$

$$\frac{\partial \epsilon}{\partial t}+U\frac{\partial \epsilon}{\partial x}+V\frac{\partial \epsilon}{\partial y}= \\ \frac{\partial}{\partial x}\left(\frac{\nu_t}{\sigma_\epsilon}\frac{\partial \epsilon}{\partial x}\right)+\frac{\partial}{\partial y}\left(\frac{\nu_t}{\sigma_\epsilon}\frac{\partial \epsilon}{\partial y}\right)+c_{\epsilon 1}\frac{\epsilon}{k}P_h+P_{\epsilon\nu}-c_{\epsilon 2}\frac{\epsilon^2}{k} \quad (27)$$

The production of turbulent energy due to the wall friction for κ and ε equations is included via the production terms:

$$P_{k\nu}=c_f^{-\frac{1}{2}}U_*^3/D \quad (28)$$

$$P_{\epsilon\nu}=c_{\epsilon T}c_{\epsilon 2}c_\mu^{\frac{1}{2}}c_f^{-\frac{3}{4}}U_*^4/D^2 \quad (29)$$

where $P_h=\nu_t|\vec{S}|^2$, $c_\mu=0.09$, $c_{\epsilon 1}=1.44$, $c_{\epsilon 2}=1.92$, $\sigma_k=1$, $\sigma_\epsilon=1.3$, $c_{\epsilon T}=-1.8$

III. CFD Simulation

In the present study only one hill in the channel was considered. The size of the hill is $x \in [-0.585, 0.585]$, $y \in [0, 0.117]$. The geometry of the hill is presented in Fig. 1.

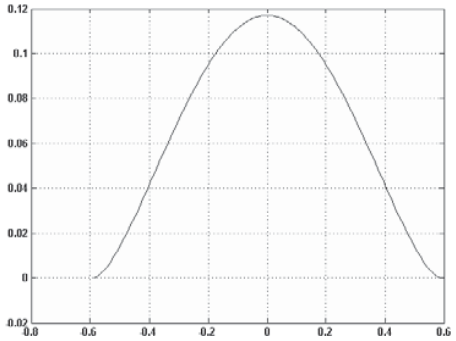

Fig. 1. Geometry of the Hill

The size of 2D domain is $x \in [-5, 5], y \in [0, 1]$ (Fig. 2).

Fig. 2. 2D geometry

Uniform wind velocity U = 1 m/s is set at the inlet and a pressure outlet condition is placed at the outlet. Periodic boundary conditions are assumed for lateral and bottom faces. The mesh of $13 * 10^3$ elements is built for 2D model. Mass and momentum sources was added to the equations by using UDF functions for 2D simulations.

Fig. 3-4 present results for $\kappa - \epsilon$ model as X velocity and static pressure.

Fig. 3. Contours of X velocity, RANS

Fig. 4. Contours of Static Pressure, RANS

The analytical solution for this model looks like:

$$U(x) = U(0)\frac{D(0)}{D(x)} \tag{30}$$

where $U(x)$ is the X velocity at point x, $U(0)$ is the initial velocity, $D(0)$ is initial depth, $D(x)$ is the depth at point x. Analytical solution for static pressure can be obtained from Bernoulli equation. Results for $\kappa - \epsilon$ model are presented in Tables I-II.

TABLE I
Results for RANS, X Velocity

X	Y	D(x)	U(x) CFD	U(x) Analytical	Error
-0.4015	0.0411	0.9589	1.04332	1.04286	0.044
-0.2538	0.0827	0.9173	1.09053	1.09015	0.035
0	0.117	0.883	1.13278	1.1325	0.025

TABLE II
Results for RANS, Static Pressure

X	Y	D(x)	P_{st} CFD	P_{st} Analytical	Error
-0.4015	0.0411	0.9589	-0.043906	-0.0483	9.1
-0.2538	0.0827	0.9173	-0.104007	-0.11	5.45
0	0.117	0.883	-0.170498	-0.1676	1.7

Results for 2D LES model are shown in Fig. 5-6.

Fig. 5. Contours of X velocity, 2D LES

Fig. 6. Contours of Static Pressure, 2D LES

Comparison with the analytical solution for 2D LES model is presented in Tables III-IV.

TABLE III
Results for 2D LES, X Velocity

X	Y	D(x)	U(x) CFD	U(x) Analytical	Error
-0.4015	0.0411	0.9589	1.04332	1.04286	0.044
-0.2538	0.0827	0.9173	1.09053	1.09015	0.035
0	0.117	0.883	1.13278	1.1325	0.025

As seen from Tables I-IV a difference with analytical solution is small, the error for 2D LES is close to 5% . The results is really satisfied taking into account the dimension was reduced on one order. They gives confidence to continue work in this direction.

TABLE IV
RESULTS FOR 2D LES, STATIC PRESSURE

X	Y	D(x)	P_{st} CFD	P_{st} Analytical	Error
-0.4015	0.0411	0.9589	-0.05097	-0.0536	4.9
-0.2538	0.0827	0.9173	-0.112778	-0.1154	2.27
0	0.117	0.883	-0.170498	-0.1731	1.5

IV. CONCLUSION

Replacing the full 3D flow by the depth-averaged equations makes it possible to save both human and CPU time. The complex 3D geometry need not be modelled nor discretized in the pre-processing state: instead, the geometry of the hill is only described with source terms in the depth-averaged equations, which are then solved in a very simple and fixed 2D domain. The method is also very fast from the point of view of a computational time, since obtaining the solution for one 2D geometry takes only few minutes. Even though the depth-averaged equations lose some 3D flow structures, they are capable of presenting the general flow behaviour with surprisingly good accuracy. Further, they speed up the design process and help in finding the most interesting geometries, which can be examined with 3D modelling and experimental pilot tests in more detail. The method introduced in this paper gives a good basis for the further development of the fast and efficient modelling of the wind park.

REFERENCES

[1] B.C. Yen, R. Camacho, R. Kohane, and B. Westrich. Signifiance of flood plains in backwater computation. *Proc. 21st Congress of IAHR*, Melbourne, pp.439-445, 1985.
[2] D. Bousmar. *Flow modelling in compound channels. Momentum transfer between main channel and prismatic or non-prismatic floodplains*. PhD thesis, Catholic University of Louvain, France, 2002.
[3] J.A. Liggett. *Fluid mechanics*. Mc Graw Hill, New-York, 1994.
[4] J. Hamalainen, T. Tiihonen. Modelling and simulation of fluid flows in a paper machine headbox. *ICIAM 95, Issue 4: Applied sciences, especially mechanics (minisymposia)* edited by E. Kreuzer, O. Mahrenholtz. pp. 62-66, Hamburg, 1995.
[5] J. Hamalainen, T. Tiihonen, E. Madetoja, H. Ruotsalainen. CFD-based optimization for a complete industrial process: Papermaking. *Optimization and Computational Fluid Dynamics* edited by D. Thevenin, G. Janiga. Springer-Verlag Berlin Heidelbrg, 2008.
[6] L. Cea, J. French, M. Vazquez-Cendon. Numerical modelling of tidal flows in complex estuaries including turbulence: An unstructured finite volume solver and experimental validation. *Internetional Journal for Numerical Methods in Engineering*, 67:1909-1932, 2006.
[7] M. Lyytikainen. *Modelling and Optimising of Chevron-type Plate Heat Exchangers*. PhD thesis, University of Kuopio, Finland, 2009.
[8] M. Lyytikainen, T. Hamalainen, J. Hamalainen. *Development of a fast modelling tool for heat exchangers based on depth-averaged equations*
[9] W. Rodi. Turbulence Models and Their Application in Hydraulics. *A State of the Art Review*. Ashgate Pub Co, 1984
[10] V. Solbakov. *Application of Mathematical Modeling for Water Environment Problems*. PhD thesis, University of Jyvaskyla, Finland, 2004.